Article

Testing Higher Derivative Gravity through Tunnelling

Ruth Gregory [1,2] **and Shi-Qian Hu** [1,*]

1   Department of Physics, King's College London, The Strand, London WC2R 2LS, UK; ruth.gregory@kcl.ac.uk
2   Perimeter Institute, 31 Caroline Street North, Waterloo, ON N2L 2Y5, Canada
*   Correspondence: shiqian.hu@kcl.ac.uk

Abstract: Higher derivative terms in the gravitational action are natural from the perspective of quantum gravity, but are perceived as leading to a lack of well-posedness. The Gauss–Bonnet term has second-order equations of motion, but does not impact gravitational dynamics in 4D, so one might expect that it is not physically relevant. We discuss how signatures can show up in tunnelling processes and whether these will likely be physically accessible in Higgs vacuum decay.

1. Brief Overview of Seeded Vacuum Decay

One of the mysteries at the core of the conflict between gravity and particle physics is the nature of the vacuum. Assumptions about the vacuum underlie Hawking radiation and inflation. But, how do we define the vacuum? The simplest way is to say it is the state of "lowest energy"; however, this presupposes that there is a lower bound and that we live in it. This research arose from re-examining the methods behind the calculations of first-order phase transitions in the universe. In nature, first-order phase transitions are usually triggered by impurities, but the classic field theory description of a first-order transition, quantum tunnelling, is more or less the opposite—extremely symmetric and idealised. How do we translate this concept of impurity to a gravitational setting, and what pitfalls arise? Further, if we go beyond Einstein's theory, how does this modify the results?

Theories of modified gravity have been developed to address some of the issues that exist in General Relativity (GR), such as late time acceleration or as an alternative to dark matter (see [1] for a review). More recently, considering modifications to GR in the strong gravitational regime provides a more-robust discriminator when testing gravity near black holes observationally. Among the alternatives to GR, higher curvature theories have a uniquely privileged position as they require no extra fundamental fields and can be motivated within a quantum gravity setting. While adding an arbitrary higher derivative term to the gravitational action can result in quartic (or higher) time derivatives, which leads to a lack of well-posedness, the Gauss–Bonnet (GB) [2–4] term (the lowest-order Lovelock contribution [5]) is quadratic in curvature while retaining only second-order field equations. A further feature of relevance to this work is the fact that a general higher curvature term will not have a Birkhoff-type theorem for the uniqueness of black hole solutions. When one has a Birkhoff theorem, the uniqueness of a black hole geometry is guaranteed. Thus, if one is performing a path integral, the geometries satisfying some given boundary constraints are now specified precisely, and one can be sure that the saddle point has been fully identified. In the absence of this uniqueness theorem, the possibility arises of multiple geometries having the same asymptotic form; hence, a background subtraction may not be unique, or even defined. Therefore, for the purpose of testing how higher curvature terms alter gravitational phenomenology in the context of vacuum decay, we focus on the GB term as an exemplar of a well-posed theory that has a Birkhoff uniqueness property [6].

The reason for being interested in vacuum decay lies in the discovery of the Higgs boson [7,8]. The measurement of Standard Model (SM) parameters, particularly the Higgs and top quark masses, reveals the possibility of a lower vacuum energy in the effective potential of the SM Higgs field at high Higgs values [9–12]. This suggests that our universe could be in a metastable vacuum that can undergo quantum tunnelling from our local minimum (false vacuum) to a global minimum (true vacuum) or exit point at a very different Higgs value. This decay is traditionally described by a process of bubble nucleation, where a bubble of true vacuum nucleates in the ambient false vacuum and, then, expands. This process was described by Coleman and collaborators [13–15] in a sequence of papers computing the tunnelling rate via so-called bounce solutions: regular solutions of the Euclidean field equations, which can, then, be readily extended to a gravitational setting using the Gibbons–Hawking [16] and Israel [17] formalisms in GR.

An alternate decay process is via the Hawking–Moss (HM) [18] instanton—a more-quantum-cosmology-motivated picture in which the universe instantaneously "jumps" to a higher vacuum energy corresponding to the (maximum) turning point of the potential, the idea being that it will then evolve cosmologically to lower, or true vacuum, energy values.

Both processes involve a Euclidean quantum gravity approach, in which the instanton is a Euclidean solution, and the leading order contribution to the probability of decay is the exponential of the tunnelling action—the difference between the initial false vacuum state and either the bounce action in the case of bubble nucleation or the higher vacuum energy universe action in the case of HM. The main difference between HM and Coleman instantons is how one interprets the transition, particularly when considering the transition to a real-time Lorentzian interpretation. The bubble nucleation picture has a natural analytic continuation back to Lorentzian (real) time, and trajectories found in the construction of the instanton rotate back to real time in a straightforward manner. The conventional interpretation is that one takes a constant τ slice of the instanton that has vanishing extrinsic curvature—i.e., is "static"—and, then, simply takes the analytically continued solution, $\tau \to -it$, with the same initial conditions at $\tau = it = 0$. The corresponding real time trajectories can be found, for example, in [19,20]. The round Euclidean bubble transforms into a hyperbolic expanding Lorentzian bubble, which rapidly expands into the false vacuum. The HM transition, however, is more fundamentally quantum. There is no analytic continuation and no "initial data surface", as the whole universe has literally jumped into a new vacuum state; rather, the new (unstable) local stationary point itself represents a new configuration of the universe that then rolls down into a new region of parameter space in a manner similar to (at least initially) the rolling of an inflationary universe.

In both the HM and bubble nucleation cases, the original computations assume the maximal symmetry of the solutions: the bubble nucleates in a constant curvature background and preserves $SO(D)$ symmetry (in D-dimensions); the HM instanton is simply the difference in action between de-Sitter (dS) solutions with different Λs. Given that first-order phase transitions in nature are typically initiated by impurities, it is clear that we need to make this picture more realistic by breaking some of these symmetries. While the general problem would require a full numerical calculation in GR, adding a black hole breaks a little of the symmetry while retaining most of the calculational control, allowing a more-general instanton to be constructed and the action computed [20–23].

Before proceeding with a summary of this picture, it is worth noting that, while quantum mechanical tunnelling is well tested and experimentally verified, quantum *field theory* tunnelling is not. As such, the approximation of taking only the suppressed exponent and the semi-classical saddle point (on which gravitational calculations rely) is based on parallels with other field theory computations, and the Euclidean approach for bubble nucleation has been challenged [24]. For the purposes of this presentation, we note these criticisms, but view analytic continuation of the "time" co-ordinate as a tool—to be used when helpful and appropriate.

1.1. Tunnelling à la Coleman

In this subsection, we review the classic picture developed by Coleman and others describing vacuum decay via the mathematical tool of analytically continuing to imaginary (Euclidean) time. Coleman's intuitive picture was to view the bubble (approximately) as a spherical bubble of true vacuum inside the false vacuum, where the bubble wall has an energy density equal to its tension. The energetics of the bubble, then, are a gain in energy from the interior being in a true vacuum, thus at lower energy than the false one, countered by the energy cost of the thin wall. We are, therefore, balancing area and volume. We can then find the instanton via a "Goldilocks" argument. Bubbles will fluctuate into existence, but if they are too small, the large surface-area- to-volume ratio causes them to re-collapse. On the other hand, while a very large bubble has a better area-to-volume ratio, the overall cost, or action, of creating it lowers the probability. There is, therefore, a "just right" size, where the action has an (unstable) stationary point— the Goldilocks bubble—which is the instanton. In terms of a formula, the energy differential is the cost of the wall less the gain in falling into true vacuum (a more-detailed derivation can be found in [13] and a heuristic discussion also including gravity in [25]):

$$\delta E = 2\pi^2 R^3 \sigma - \frac{\pi^2}{2}\varepsilon R^4 \tag{1}$$

where σ is the tension of the wall and ε is the difference in energy between the true and false vacuum, assumed small. This energy shift is stationary at $R = 3\sigma/\varepsilon$, which corresponds beautifully to a calculation of the full Euclidean field equations. Substituting this value of R at the stationary point of (1) gives the bounce action as

$$\mathcal{B} = \frac{\pi^2 R^3}{2}(4\sigma - \varepsilon R) = \frac{27\pi^2 \sigma^4}{2\varepsilon^3} \tag{2}$$

which then gives the leading-order, or saddle point, contribution to the amplitude for tunnelling $\mathcal{P} \sim e^{-\mathcal{B}}$.

Of course, this is not the full story: energy gravitates; therefore, we should include the impact of an infinite volume of false vacuum. This was worked out in the paper of Coleman and de Luccia (CDL) [15] using the thin wall approximation described above. As before, the instanton is a solution of the Euclidean Einstein equations with a spherical bubble separating true and false vacuum solutions. Computing quantum processes with gravity is always delicate, as we do not have a consensus on a working theory of quantum gravity. Here, we will be taking the partition function approach of Gibbons and Hawking [16] and work within the saddle point approximation. It is worth noting that this focus on the gravitational side of the problem does not address questions such as thermal corrections to the scalar (Higgs) potential.

The gravitational action with a thin wall is

$$S_E = -\frac{1}{16\pi G}\int_{\mathcal{M}_+ \cup \mathcal{M}_-} d^4x \sqrt{g}(R - 2\Lambda) + \frac{1}{8\pi G}\int_{\partial\mathcal{M}_+ \cup \partial\mathcal{M}_-} d^3x \sqrt{h}K + \int_{\mathcal{W}} d^3x \sqrt{h}\sigma \tag{3}$$

and the CDL procedure is to construct a geometry that interpolates between the true and false vacua across the wall, using the Israel junction conditions to calculate the wall trajectory. To illustrate briefly, consider tunnelling from positive (false) to zero (true) vacuum energy. A Euclidean de-Sitter space has the geometry of a four-sphere with radius $\ell = \sqrt{3/8\pi G\varepsilon}$, and zero vacuum energy is just flat Euclidean $\mathbb{R}^4$:

$$ds^2 = \begin{cases} d\rho^2 + \ell^2 \sin^2(\rho/\ell)d\Omega_{III}^2 & \text{false (de-Sitter)} \\ dr^2 + r^2 d\Omega_{III}^2 & \text{true} \end{cases} \tag{4}$$

The polar coordinates are chosen to centre on the wall, which sits at $r_0 = \ell \sin(\rho_0/\ell) = R$, which has an induced metric:

$$h_{ab} = g_{ab} - n_a n_b \tag{5}$$

where the normal n_a is proportional to $d\rho$ or dr. The energy momentum of the wall is σh_{ab}, which is related to the jump in extrinsic curvature via the Israel junction conditions:

$$K_{ab}^+ - K_{ab}^- = -\frac{1}{R}\left(1 - \sqrt{1 - \frac{R^2}{\ell^2}}\right)h_{ab} = -4\pi G\sigma h_{ab} \tag{6}$$

Writing $\bar{\sigma} = 2\pi G\sigma$, this is solved by

$$R_0 = \frac{4\bar{\sigma}\ell^2}{1 + 4\bar{\sigma}^2\ell^2} \tag{7}$$

which can, then, be substituted into the Euclidean action to obtain

$$\mathcal{B}_{CDL} = S_E(\text{instanton}) - S_E(dS) = \frac{\pi\ell^2}{G}\frac{16\bar{\sigma}^4\ell^4}{(1 + 4\bar{\sigma}^2\ell^2)^2} \tag{8}$$

Noting the expressions for ℓ and $\bar{\sigma}$, we see that this expression

$$\mathcal{B}_{CDL} = \frac{27\pi^2\sigma^4}{2\varepsilon^3(1 + 6\pi G\sigma^2)^2} \tag{9}$$

has the correct $G \to 0$ limit (2).

1.2. Seeded Tunnelling

The description of tunnelling given above is extremely idealised with maximal symmetry and no inhomogeneity; however, most first-order phase transitions are triggered by impurities in the system. Taking this idea on board, Refs. [20–23] considered a gravitational impurity, in the guise of a black hole, that breaks the maximal symmetry, but retains enough symmetry to allow analytic analysis in the case of the thin wall. Black-hole-seeded tunnelling in Einstein gravity is recapped in this subsection to set the stage for the inclusion of the GB term. We show the comparison rate between Hawking evaporation and tunnelling, as well as the HM instanton.

The instanton geometry now becomes that of a thin wall solution interpolating between two different Schwarzschild black holes with different cosmological constants. The problem of finding the geometry of a wall in the presence of a bulk black hole reduces to a Birkhoff theorem, which was first generalised to arbitrary Λ and black hole curvature in [26] (and arbitrary dimension in [27]), where a domain wall was also included in the analysis. The integrability of the vacuum Einstein equations shows that the general solution is comprised of two exact Schwarzschild (A/dS) geometries separated by a domain wall, which follows a possibly dynamical trajectory $R(\lambda)$ centred with respect to the black holes.

$$ds^2 = \begin{cases} f_+(r)d\tau_+^2 + \frac{dr^2}{f_+(r)} + r^2 d\Omega_{II}^2 & R > R(\lambda) \\ f_-(r)d\tau_-^2 + \frac{dr^2}{f_-(r)} + r^2 d\Omega_{II}^2 & R < R(\lambda) \end{cases} \tag{10}$$

with

$$f_\pm(r) = 1 - \frac{2M_\pm}{r} - \frac{\Lambda_\pm}{3}r^2 \tag{11}$$

It is straightforward to find solutions to the Israel junction conditions, and typically, for each seed mass M_+, there is an allowed range for M_- for the given vacuum energy differ-

ential. Although the methodology for computing the action is slightly distinct depending on the sign of Λ, the final result for the instanton action is relatively simple [21]:

$$\mathcal{B} = \frac{\mathcal{A}_+}{4G} - \frac{\mathcal{A}_-}{4G} + \frac{1}{4G} \oint d\lambda \left\{ \left(2Rf_+ - R^2 f'_+\right) \dot{\tau}_+ - \left(2Rf_- - R^2 f'_-\right) \dot{\tau}_- \right\} \tag{12}$$

It is, then, easy to see that, for each M_+, there is a unique M_- that minimises this action, hence dominates the tunnelling amplitude. In [21], it was shown that, for small M_+, this minimal M_- vanishes; hence, these instantons are perturbed CDL bubbles, whereas, for larger M_+, there is a remnant black hole, with a mass determined by M_+, Λ_+ and Λ_-, this latter instanton being independent of Euclidean time. As a static solution, the action of these instantons is particularly simple and is just the entropy change in the geometry:

$$\mathcal{B}_s = S_+ - S_- \tag{13}$$

which corresponds neatly to a Boltzmann suppression for a tunnelling that decreases entropy.

In [20,22,23], the thick wall versions of these instantons were constructed numerically to explore the impact on Higgs vacuum tunnelling, with the result that the black hole could potentially drastically increase the probability of vacuum decay. In the case of a black-hole-seeded phase transition, the key comparison is with the rate of evaporation of the black hole, which is proportional to $1/M^3$, thus might be expected to be dominant at all scales; however, the prefactor of this power law, computed by Page [28], is suppressed, so the question is more subtle. In fact, when computing the area difference between seed and remnant black holes, the mass screened by the thick Higgs bubble is significantly less than the mass of the seed black hole, so the entropy difference is, to a good approximation,

$$\mathcal{B} = \pi(r_s^2 - r_r^2) \sim 4\pi(M_s + M_r)(M_s - M_r) = 8\pi M_s \delta M \tag{14}$$

Estimating the instanton prefactor using the scale of the black hole seed gives this branching ratio as [25]

$$\frac{\Gamma_D}{\Gamma_H} \sim 88 M^{3/2} \sqrt{\pi \delta M} e^{-4\pi M \delta M} \tag{15}$$

which is sketched in Figure 1 and corresponds well with the figures in [20,23], which were obtained by numerical evaluation.

Finally, an alternate description of vacuum decay is given by the HM [18] instanton. This type of decay applies to potentials that have a very flat barrier to decay, and the transition occurs from the local false vacuum minimum to the top of the potential barrier, from which the universe can roll to lower true vacua. The HM rate is, then, given by $\Gamma_{F \to T} \sim e^{-B}$, where B is simply the difference in the Euclidean actions of the two vacuum de-Sitter spacetimes:

$$I_{HM} = I_T - I_F = S_F - S_T = \frac{\pi}{G} \left[\ell_F^2 - \ell_T^2 \right] \tag{16}$$

which, again, is a Boltzmann factor related to the drop in entropy incurred by the cosmological horizon area decreasing. The corresponding process for the black hole Hawking–Moss (BHHM) instantons was considered in [29,30], where the action includes the black hole horizon:

$$B_{F \to T} = I_T - I_F = [S_{CH} + S_{BH}]_F - [S_{CH} + S_{BH}]_T . \tag{17}$$

By using the reparametrisation:

$$r_c = \frac{2}{\sqrt{3}} \ell \cos\left(\frac{\pi}{3} - b\right), \quad r_h = \frac{2}{\sqrt{3}} \ell \cos\left(\frac{\pi}{3} + b\right), \quad b = \frac{1}{3} \cos^{-1}\left(\frac{3\sqrt{3}GM}{\ell}\right). \tag{18}$$

the BHHM transition action can be compactly expressed as

$$B = \pi \left[\frac{4}{3}\left(\ell_F^2 - \ell_T^2\right) - \frac{2}{3}\ell_F^2 \cos(2b_F) + \frac{2}{3}\ell_T^2 \cos(2b_T) \right] \tag{19}$$

So, for example, as M runs from 0 to its Nariai maximum $\ell/3\sqrt{3}$, b drops from $\pi/6$ to 0 and the action drops from $\pi\ell^2$ to $2\pi\ell^2/3$. It is, therefore, easy to see that, in tunnelling from a black hole seed to a pure de-Sitter state, the action drops; therefore, black holes increase the probability of a transition. The full details can be found in [30].
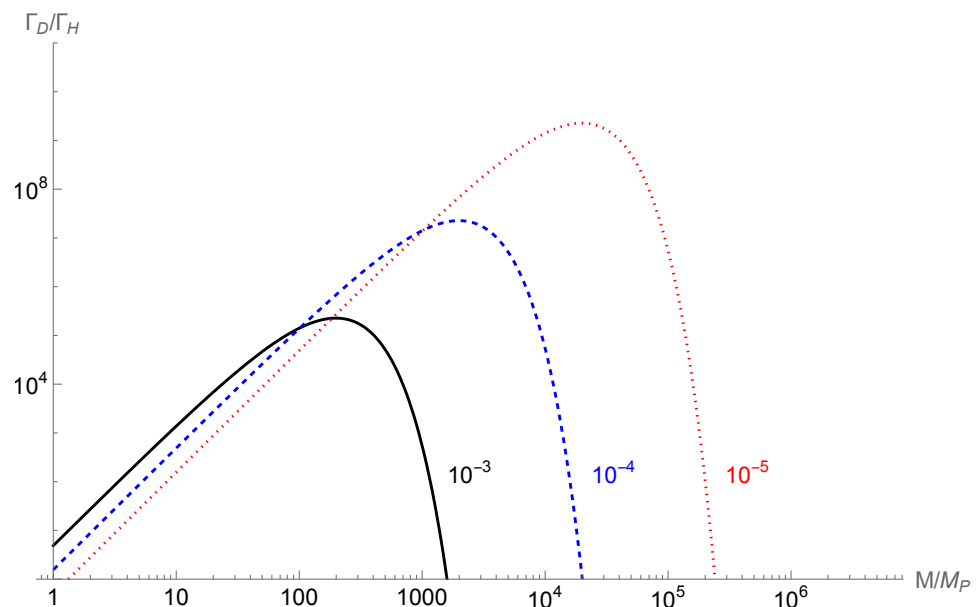

Figure 1. The approximation for Γ_D/Γ_H as given in (15) as a function of seed mass for the differential seed ratio masses indicated.

2. Seeded Decay in Einstein Gauss–Bonnet Gravity: Bubble Nucleation

While most of the phenomenologically relevant computations for vacuum decay have been discussed in four spacetime dimensions, it is also interesting to consider how extra dimensions can impact vacuum decay. General considerations of how large extra dimensions could impact black hole seeded vacuum decay were explored in [23,31,32] for both noncompact and braneworld-type scenarios in the context of Einstein gravity. However, allowing for the dimensionality of spacetime to be arbitrary raises the possibility of including higher curvature terms in the action. Here, we focus on the addition of the GB term [2–4] as it is the lowest-order Lovelock term [5], which still retains second-order equations of motion. Further, since the computation of instanton actions frequently involves a background subtraction, we require a Birkhoff-type theorem, so that we know that the relevant background is unique. The Lovelock terms satisfy this condition, whereas generic higher-order terms do not (as well as typically suffering from a lack of well-posedness). In 4D, the GB term is a topological invariant and does not alter the dynamics of the theory; however, it can potentially change the action, hence is of relevance to a tunnelling process, where the action determines the probability of decay. We first briefly review the derivation of the equations of motion from [33] before extending the discussion to include dynamical bubbles. By expanding in the GB parameter, α, we are able to show that the equations of motion can be re-cast in the same form as the Einstein equations of motion, albeit with different details in the coefficients. We recap the computation of the action, then discuss a test case example in arbitrary dimensions in detail, discussing the impact of the α term. We finally comment on a peculiarity of EGB black holes in 5D, namely the presence of a "mass gap" in the black hole family of solutions.

2.1. Seeded Bubbles in Einstein-Gauss–Bonnet

The gravitational action of Einstein-Gauss–Bonnet (EGB) gravity is

$$I = -\frac{1}{16\pi G} \int_{\mathcal{M}} d^D x \sqrt{g} [\mathcal{R} - 2\Lambda + \alpha \mathcal{L}_{GB}]$$
$$\mathcal{L}_{GB} = R^2 - 4R_{ab}^2 + R_{abcd}^2 \tag{20}$$

where α is a dimensionful coupling constant, here taken to be positive. As in the pure Einstein case described previously, we look for bubble trajectories in the thin wall approximation, where the vacuum transitions completely and instantaneously across the wall, as this will capture the impact of the additional GB term on the process.

As before, there is a Birkhoff theorem for EGB gravity in the presence of a brane [6,34,35], and the brane junction conditions were discussed in [36], although were only explicitly derived for $\mathbb{Z}_2$ symmetry across the wall. The bubble spacetime is again a wall separating two spherical vacuum solutions with a seed and remnant mass black hole as in (10), but with $d\Omega_{II}^2 \rightarrow d\Omega_{D-2}^2$ as appropriate for a higher-dimensional solution and with the metric potential now [37–39].

$$f_{\pm} = 1 + \frac{r^2}{2\tilde{\alpha}} \left(1 - \sqrt{1 + \frac{8\tilde{\alpha}\Lambda_{\pm}}{(D-1)(D-2)} + \frac{4\tilde{\alpha}\mu_{\pm}}{r^{D-1}}} \right), \tag{21}$$

with $\tilde{\alpha} = (D-3)(D-4)\alpha$ and μ related to the mass through the Myers–Perry formula [40]:

$$\mu = \frac{16\pi G M}{(D-2)\mathcal{A}_{D-2}}, \tag{22}$$

and $\mathcal{A}_{D-2}$ being the area of a unit $(D-2)-$sphere.

The action of the bubble is the sum of the parts from the bulk on each side given by (20) together with the wall piece, including both the wall tension and the geometrical Gibbons–Hawking-type terms, which now include additional EGB contributions [36,41]:

$$I_{brane} = \int_{brane} d^{D-1} x \sqrt{h} \left(\sigma + \frac{1}{8\pi G} \left(\Delta K - 2\alpha \left[2\mathcal{G}_{ab}\Delta K^{ab} - \Delta\mathcal{J} \right] \right) \right) \tag{23}$$

where $\mathcal{J}$ is the cubic extrinsic tensor:

$$\mathcal{J}_{ab} = \frac{1}{3} \left(2KK_{ac}K_b^c + K_{cd}K^{cd}K_{ab} - 2K_{ac}K^{cd}K_{db} - K^2 K_{ab} \right). \tag{24}$$

The generalised Israel junction conditions at the wall are obtained by varying this action:

$$\Delta K_{ab} - \Delta K h_{ab} + 2\alpha \left[3\Delta\mathcal{J}_{ab} - \Delta\mathcal{J} h_{ab} - 2\mathcal{P}_{acbd}\Delta K^{cd} \right] = 8\pi G\sigma h_{ab} \tag{25}$$

with

$$\mathcal{P}_{abcd} = \mathcal{R}_{abcd} + 2\mathcal{R}_{b[c}h_{d]a} - 2\mathcal{R}_{a[c}h_{d]b} + \mathcal{R}h_{a[c}h_{d]b} \tag{26}$$

the divergence-free part of the intrinsic Riemann tensor. The equations of motion, while simple for a spacetime reflection symmetric around the wall now become far more involved when we have the situation of a false–true vacuum and the interior–exterior of the bubble. Writing the general wall trajectory as $R(\lambda)$ and computing the extrinsic and intrinsic curvatures, (25) becomes

$$-\frac{8\pi G\sigma R}{(D-2)} = -2\bar{\sigma}R = \left(\sqrt{f_+ - \dot{R}^2} - \sqrt{f_- - \dot{R}^2} \right) \left[1 + \frac{2\tilde{\alpha}}{R^2} - \frac{4\tilde{\alpha}}{3}\frac{\dot{R}^2}{R^2} \right]$$
$$- \frac{2\tilde{\alpha}}{3R^2} \left(f_+\sqrt{f_+ - \dot{R}^2} - f_-\sqrt{f_- - \dot{R}^2} \right) \tag{27}$$

As with the Einstein case, this equation can be manipulated into a Friedmann-like equation for R, which is most compactly written in terms of the variable $X = (1 - \dot{R}^2)/R^2$ [33]:

$$
\begin{aligned}
0 = {} & \tilde{\alpha}^2 X^3 + \tilde{\alpha} X^2 \left(\frac{1}{6} - \frac{(S_+^2 - S_-^2)^2}{256\tilde{\alpha}\bar{\sigma}^2} \right) \\
& + \frac{X}{4} \left(3 - \frac{3(S_+^2 + S_-^2)}{8} - \frac{(S_+^2 - S_-^2)(3S_+^2 - 3S_-^2 + S_+^3 - S_-^3)}{192\tilde{\alpha}\bar{\sigma}^2} \right) \\
& + \frac{(8 - 3S_+^2 - 3S_-^2 - S_+^3 - S_-^3)}{64\tilde{\alpha}} - \frac{(3S_+^2 - 3S_-^2 + S_+^3 - S_-^3)^2}{9216\tilde{\alpha}^2\bar{\sigma}^2} - \frac{9\bar{\sigma}^2}{16}
\end{aligned}
\tag{28}
$$

where, for compactness of notation, we introduce

$$
S_\pm = \sqrt{1 + \frac{8\tilde{\alpha}\Lambda_\pm}{(D-1)(D-2)} + \frac{4\tilde{\alpha}\mu_\pm}{r^{D-1}}} = \sqrt{1 + \frac{4\tilde{\alpha}}{r^2}(1 - f_{\pm E})}
\tag{29}
$$

which is related to the standard Einstein potential $f_E = 1 - \mu/r^{D-3} - 2\Lambda r^2/(D-1)(D-2)$.

While one can in principle solve the cubic (28) to find the solution for X (by identifying the root that is connected to the Einstein solution as $\alpha \to 0$), it proves useful to identify the $\mathcal{O}(\alpha)$ correction to the trajectories by expanding (28) in $\tilde{\alpha}$ to obtain a Friedmann-like equation for R:

$$
\frac{\dot{R}^2}{R^2} = \frac{\bar{f}_E}{R^2} - \frac{(\Delta f_E)^2}{16R^4\bar{\sigma}^2} - \bar{\sigma}^2 + \frac{\tilde{\alpha}}{3R^4} \left\{ 3(\bar{f}_E - 1)^2 + \frac{(\Delta f_E)^2}{4} + 12R^2\bar{\sigma}^2(1 - \bar{f}_E) + 8R^4\bar{\sigma}^4 \right\}
\tag{30}
$$

where $\bar{f}_E = (f_+ + f_-)/2$.

Note that both this $\mathcal{O}(\alpha)$ equation, as well as the original cubic in X are quadratic in $\dot{R}$. This means that, to obtain the real time evolution of the bubble once it has nucleated, we simply analytically continue back to Lorentzian time, $\tau \to -it$, to determine the real time evolution of the bubble. A "round" Euclidean bubble will correspond to a hyperbolic Lorentzian solution, where the bubble starts to expand upon formation. A "static" Euclidean bubble will nucleate to an initially static Lorentzian bubble, but this is an unstable configuration, so we expect that, on average, half of these bubbles will, then, expand to complete the phase transition.

From (30), we can manipulate the equation of motion for R in a fashion similar to [21], where the effective scale of R was defined in terms of parameters γ and a (the notation of [21] was α, which we have modified here to avoid confusion). To include the GB parameter α, define:

$$
\bar{\sigma}_e^2 = \bar{\sigma}^2(1 - 8\tilde{\alpha}\bar{\sigma}^2/3) , \quad \frac{1}{\ell_e^2} = \frac{2\Delta\Lambda(1 - 4\tilde{\alpha}\bar{\sigma}^2)}{(D-1)(D-2)} , \quad \gamma_e = \frac{4\bar{\sigma}_e\ell_e^2}{1 + 4\bar{\sigma}_e^2\ell_e^2} ,
\tag{31}
$$

and

$$
a^2 = 1 + \frac{2\Lambda_-\gamma_e^2}{(D-1)(D-2)} \left[1 - 4\tilde{\alpha}\bar{\sigma}^2 - \frac{2\Lambda_+\tilde{\alpha}}{(D-1)(D-2)} \right]
\tag{32}
$$

Now, defining $\hat{R} = aR/\gamma_e$ and $\hat{\lambda} = a\lambda/\gamma_e$, the equation of motion takes the form:

$$
\left(\frac{d\hat{R}}{d\hat{\lambda}} \right)^2 = 1 - \left(\hat{R} + \frac{\hat{C}}{\hat{R}^{D-2}} \right)^2 - \frac{\hat{B} - 2\hat{C}}{\hat{R}^{D-3}}
\tag{33}
$$

where

$$\hat{B} = \left(\frac{a}{\gamma_e}\right)^{D-3}\left[\bar{\mu}\left(1 - 4\tilde{\alpha}\bar{\sigma}^2 - \frac{4\bar{\Lambda}\tilde{\alpha}}{(D-1)(D-2)}\right) + \frac{\Delta\mu}{8\bar{\sigma}_e^2\ell_e^2}\right]$$
$$\hat{C} = \left(\frac{a}{\gamma_e}\right)^{D-2}\left[\frac{(\Delta\mu)(1 - 4\tilde{\alpha}\bar{\sigma}^2)}{4\bar{\sigma}_e} - 2\tilde{\alpha}\frac{\mu_+\mu_-\bar{\sigma}_e}{\Delta\mu}\right]$$

(34)

This format is the same as for the Einstein case, although the coefficients are corrected by $\tilde{\alpha}$; thus, the principle for solving the instanton equations is the same. The qualitative picture, of the preferred instanton being a modified CDL bubble with a black hole seed, but no remnant for a small mass, and a static instanton with a remnant black hole for larger masses remains; however, the relation between the seed and remnant masses will be modified by $\tilde{\alpha}$.

2.2. Bubble Actions

While the general cubic equation for X is algebraically involved, we can still derive an expression for the action of a general instanton in terms of the wall trajectory $R(\lambda)$, then specialise to the case where $R(\lambda) = R_0$ is constant. We also expect that the ratio γ_e/a will still broadly represent the scale of the wall motion.

To compute the action, the procedure is the same as for the Einstein case, where we first compute the action of the background (seed) geometry with the proviso that we compute at an arbitrary periodicity of Euclidean time, so that we can match to the exterior of the bubble spacetime. As with the Einstein instanton, this shifting of periodicity means we have to regularise the resulting conical deficit at the horizon, a procedure detailed in [33]. The result is that we can write the seed action as

$$I_{seed} = I_c - S_{BH}(M_+).$$

(35)

where S_{BH} is the entropy of the black hole

$$S_{BH} = \frac{\mathcal{A}_{D-2}r_h^{D-2}}{4G}\left(1 + \frac{2(D-2)\tilde{\alpha}}{(D-4)r_h^2}\right)$$

(36)

and I_c represents a "large r" contribution, which depends on the asymptotic structure of the spacetime. While we do not need to know its exact form, as this term will be the same for both bubble and seed spacetimes, its general form is:

$$I_c = \begin{cases} \frac{\beta\mathcal{A}_{D-2}}{16\pi G}r_c^{D-4}f'(r_c)\left(r_c^2 + \frac{2(D-2)\tilde{\alpha}}{(D-4)}(1 - f(r_c))\right) & \Lambda \leq 0 \\ -S_{cos} & \Lambda > 0 \end{cases}$$

(37)

For the bubble geometry, the fact that the bulk integral (20) reduces to a total derivative on shell means that it only contributes an entropy term at the black hole horizon r_h, the same term as the seed at the large r cutoff r_c, together with contributions evaluated on each side of the wall:

$$I_{bulk,\mathcal{W}} = -\frac{\mathcal{A}_{D-2}}{16\pi G}\int d\lambda R^{D-4}\left[f'_+\dot{t}_+\left(R^2 + \frac{2(D-2)\tilde{\alpha}}{(D-4)}(1 - f_+)\right)\right.$$
$$\left. - f'_-\dot{t}_-\left(R^2 + (1 - f_-)\right)\right].$$

(38)

Meanwhile, the wall integral (23) can be manipulated using the trace of the Israel equations to give

$$I_{\mathcal{W}} = \frac{\mathcal{A}_{D-2}}{8\pi G}\int d\lambda\frac{R^{D-2}}{(D-1)}\left(\Delta K - \frac{6\tilde{\alpha}}{(D-3)(D-4)}\left[2\mathcal{G}_{ab}\Delta K^{ab} - \Delta\mathcal{J}\right]\right).$$

(39)

Giving the total wall contribution as

$$I_{wall} = \frac{\mathcal{A}_{D-2}}{8\pi G} \int d\lambda R^{D-2} \Delta \left[-\frac{4(D-2)\tilde{\alpha}}{(D-4)} \frac{\dot{R}}{R} K_1 + \left(\frac{\dot{R}^2}{f} K_0 - \dot{t}\ddot{R} \right) \left(1 + \frac{2(D-2)\tilde{\alpha}(1-f)}{(D-4)R^2} \right) \right]. \quad (40)$$

Pulling together all these formulae, the instanton action is computed as

$$I_{\mathcal{B}} = I_{bubble} - I_{seed} = S_{BH}(M_+) - S_{BH}(M_-) + I_{wall}. \quad (41)$$

In other words, as with Einstein gravity, the instanton action consists of an entropy differential together with a dynamical wall integral, which was shown in [33] to vanish for the static instanton. Thus, as for Einstein gravity, the dominant decay process for most black holes is the static instanton and has a probability of

$$\mathcal{P} \sim exp[-(S_{seed} - S_{remnant})/\hbar] \quad (42)$$

In 4D, although the GB term has a vanishing contribution to the gravitational dynamics, it does change the action of a solution due to the modified expression for entropy:

$$S_{BH} = \frac{\pi r_+^2}{G} \left(1 + \frac{4\alpha}{r_+^2} \right) = \frac{\pi r_+^2}{G} + \frac{4\pi\alpha}{G} \quad (43)$$

This constant shift is not relevant for the thermodynamics of the black hole [42], and if tunnelling from a seed to a remnant black hole, these terms will cancel; however, if we have a topology-changing process such as tunnelling from a seed to no remnant, then this term will be relevant. Thus, since it is possible to show that a bubble cannot nucleate with a black hole inside from a pure false vacuum [33], this term always suppresses topology-changing transitions.

In higher dimensions, the GB parameter will modify the wall trajectory, as well as the action, so in order to extract the impact of the GB correction, we will explore how the critical static bubble is impacted by α. The critical static bubble is the instanton with the lowest action for a given wall tension σ. It connects the modified CDL branch, which represents the preferred instanton at very low seed masses, where the interior of the bubble has no black hole, to the static branch, where there is both a seed and remnant black hole; the critical instanton is, therefore, static, but has no remnant, and the seed mass is fully determined by the vacuum energies and wall tension.

For simplicity, we will explore tunnelling from a positive vacuum energy with the seed black hole to the Minkowski vacuum. Therefore, $\Delta\mu = \mu_+ = 2\bar{\mu}$, and $\Delta\Lambda = \Lambda_+ = 2\bar{\Lambda}$. Thus, $a = 1$, and the parameters in (33) simplify to

$$\hat{B} = \frac{\mu_+ (1 - 4\tilde{\alpha}\bar{\sigma}^2)}{2\bar{\sigma}_e \gamma_e^{D-2}} = 2\hat{C} \quad (44)$$

Thus, the static instanton constraints read

$$1 = \left(\hat{R} + \frac{\hat{C}}{\hat{R}^{D-2}} \right)^2$$
$$0 = 2 \left(\hat{R} + \frac{\hat{C}}{\hat{R}^{D-2}} \right) \left(1 - (D-2) \frac{\hat{C}}{\hat{R}^{D-1}} \right) \quad (45)$$

identical in form to the Einstein case. These are solved by

$$\hat{C} = \frac{(D-2)^{D-2}}{(D-1)^{D-1}} \quad ; \qquad \hat{R} = \frac{(D-2)}{(D-1)} \quad (46)$$

Hence,

$$\mu_{crit} = \frac{4\bar{\sigma}_e \gamma_e^{D-2}}{(1 - 4\tilde{\alpha}\bar{\sigma}^2)} \frac{(D-2)^{D-2}}{(D-1)^{D-1}} \tag{47}$$

from which one can see that the critical instanton seed mass increases with $\tilde{\alpha}$ by expanding the expressions for the effective parameters $\bar{\sigma}_e, \gamma_e$:

$$\frac{\delta\mu_{crit}}{\mu_0} = \frac{8}{3}\tilde{\alpha}\bar{\sigma}^2[1 + (D-2)(1 - 2\bar{\sigma}\gamma_0)] \tag{48}$$

where the subscript "0" indicates the values of the various functions at $\tilde{\alpha} = 0$ and μ_0 is the critical mass at $\tilde{\alpha} = 0$:

$$\mu_0 = \frac{(4\bar{\sigma}\ell_0)^{D-1}\ell_0^{D-3}}{(1 + 4\bar{\sigma}^2\ell_0^2)^{D-2}} \frac{(D-2)^{D-2}}{(D-1)^{D-1}} \tag{49}$$

However, the instanton action is determined by the entropy of the seed mass, which, in turn, is determined by the horizon radius, which actually *decreases* as $\tilde{\alpha}$ is switched on. Thus, the actual incremental change in the action is a combination of these effects and further complicated by the nature of the polynomial determining the horizon in the various dimensions. Computing the incremental change in the horizon radius and critical mass, we arrive at an expression for the entropy shift at small $\tilde{\alpha} \lesssim \mu_0^{2/(D-3)}$:

$$\frac{\delta S}{S_0} = \frac{(D-2)\tilde{\alpha}}{r_0^3 f_E'(r_0)} \left(\frac{2r_0 f_E'(r_0)}{(D-4)} + \frac{8\mu_0\bar{\sigma}^2}{3r_0^{D-5}}[1 + (D-2)(1 - 2\bar{\sigma}\gamma_0)] - 1 \right) \tag{50}$$

The shift in entropy is proportional to $\tilde{\alpha}$, as expected; the other key dependence is on $\bar{\sigma}\ell_0$, which, in turn, feeds into μ_0. As discussed in [22], $2\bar{\sigma}\gamma_0 < 1$; hence, the critical mass becomes very strongly damped for low $\bar{\sigma}\ell$ at large D; hence, the range of $\tilde{\alpha}$ for which (50) is relevant becomes small. This is reflected in the range for $\tilde{\alpha}\ell_0^2$ in Figure 2.

Exploring the entropy change (50) for various D shows that the shift in entropy with $\tilde{\alpha}$ is positive. Thus, the GB term lowers the tunnelling amplitude. The picture for 5D is more nuanced, however. In 5D, the horizon radius can be simply found as

$$r_h = \frac{\ell_0}{\sqrt{2}} \left(1 - \sqrt{1 + \frac{4(\tilde{\alpha} - \mu)}{\ell_0^2}} \right)^{1/2} \tag{51}$$

Clearly, $r_h \to 0$ as $\mu \to \tilde{\alpha}$, i.e., at finite values of μ_{crit}; hence, $\bar{\sigma}$, and there is no horizon for $\mu < \tilde{\alpha}$. Thus, we have an interesting "mass gap" in the 5DGB black hole family. Spacetimes with $\mu < \tilde{\alpha}$, i.e., ADM mass below $3\pi\alpha/4G$, do not have a horizon, but instead have a solid angle deficit as $r \to 0$. This phenomenon has been noticed in the study of gravitational collapse in EGB gravity [43–45]. This makes 5D crucially different from higher dimensions, in that, while the entropy of the seed does initially increase with $\tilde{\alpha}$, for low $\bar{\sigma}\ell_0$, we see that the entropy function (calculated exactly, rather than using (50)) turns over and decreases, eventually dropping to zero as this mass limit is hit. We, therefore, expect that the semi-classical approximation should not be valid for small seed black holes.

In Figure 2, we show the variation in entropy of the seed black hole (which directly translates into the instanton action) as $\tilde{\alpha}$ is switched on for both 5 and 6 dimensions. Although the generic picture is that the entropy increases as $\tilde{\alpha}$ increases, the one exception is for $D = 5$ and smaller $\bar{\sigma}$. As discussed above, caution should be used in pushing to too low a $\bar{\sigma}$.
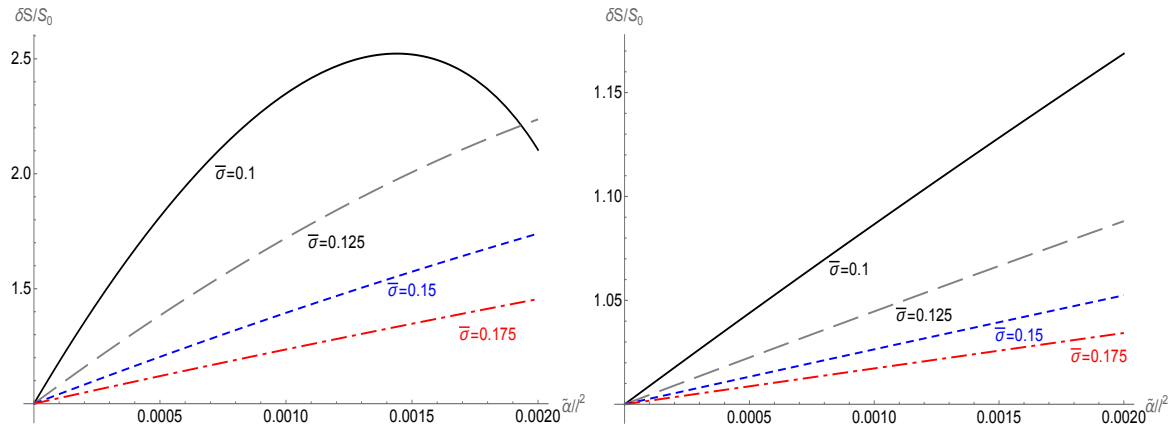
Figure 2. The shift in entropy of the critical instanton in 5 (**left**) and 6 (**right**) dimensions as a function of $\tilde{\alpha}/\ell^2$ for the given bubble wall tensions indicated, $\bar{\sigma} = 0.1, 0.125, 0.15, 0.175$, respectively.

3. Seeded Decay in Einstein Gauss–Bonnet Gravity: Hawking–Moss

In this section, we briefly review Hawking–Moss tunnelling with a GB term [33], expanding on the distinctiveness of the 5D results. The HM instanton is a transition from a false vacuum to a higher vacuum energy, from which the universe can roll to lower true vacua. While it is not possible to tunnel from no black hole to a black hole for bubbles, this can happen for BHHM transitions.

The HM and BHHM transition probabilities are easy to compute, as one is comparing the actions for Schwarzschild GB de-Sitter geometries, where the cosmological constants are determined by the vacuum energy in the false vacuum (denoted by the subscript F) and the vacuum energy at the local maximum of the potential (denoted T) that the universe instantaneously jumps to in this transition. The action of a Schwarzschild GB dS geometry was shown in the previous section to be

$$I_{SGBDS} = -S_{CH} - S_{BH} \tag{52}$$

i.e., minus the sum of the entropies of the cosmological and black hole horizons; thus, the tunnelling rate, dominated by the Boltzmann factor, $\Gamma_{F \to T} \sim e^{-B}$, is given by

$$
\begin{aligned}
B_{F \to T} = I_T - I_F &= [S_{CH} + S_{BH}]_F - [S_{CH} + S_{BH}]_T \\
&= \frac{\mathcal{A}_{D-2}}{4G} \Big[r_{CF}^{(D-2)} + r_{BF}^{(D-2)} - r_{CT}^{(D-2)} - r_{BT}^{(D-2)} \\
&\quad + \frac{2(D-2)\tilde{\alpha}}{(D-4)} \Big(r_{CF}^{(D-4)} + r_{BF}^{(D-4)} - r_{CT}^{(D-4)} - r_{BT}^{(D-4)} \Big) \Big]
\end{aligned}
\tag{53}
$$

where (for example) r_{CT} stands for the cosmological horizon radius of the nucleated universe at the top of the potential and r_{BT} for the black hole horizon radius in the seed universe.

In general, in 4D, the GB term does not affect the BHHM transition; however, it will suppress tunnelling from a black hole seed to a pure GB de-Sitter state. This gives a lack of continuity in the most-likely instanton, where tunnelling to an infinitesimally small mass black hole is preferred over tunnelling to the pure vacuum, although one should not apply this semi-classical approach for black holes around the Planck scale. On the other hand, note that, now, tunnelling from a pure de-Sitter false vacuum to a Schwarzschild–de-Sitter (SdS) spacetime at the top of the potential is allowed as an HM transition. For these (topology-changing) configurations, the action is now lowered by $\delta I \sim 4\alpha/G - 2\pi \ell M$ relative to the pure (black-hole-free) HM transition; thus, again, there is a preferred transition to a vanishingly small mass black hole universe. While one might imagine that this small black hole would rapidly evaporate, there is a conflict in constructing a semi-classical solution with a Planckian-scale black hole.

In higher dimensions, the impact of seeded decay in BHHM transitions can be computed straightforwardly from (53) (once the horizon radii are found), and the results are shown in Figures 3 and 4 for 5D and 6D, respectively. An interesting feature appears in 5D due to the "mass gap" for black hole solutions. As already noted, in $D = 5$, there is a lower limit to the mass a *black hole* can have, as the horizon radius $r_h \rightarrow 0$ as $M \rightarrow 3\pi\alpha/4G$. Below this mass, the solution does not have a horizon, but, instead, contains a solid angle deficit as $r \rightarrow 0$. This causes the dependence of the HM tunnelling amplitude with seed mass to have a discontinuity in its derivative (though it is doubtful this is physically relevant).

Looking in a bit more detail, the black hole horizon radius is given by (51), where $\tilde{\alpha} = 2\alpha$ and $\mu = 8GM/3\pi$. Thus, as the critical mass $M_C = 3\pi\alpha/4G$ is approached, the black hole horizon radius vanishes as

$$r_b \sim \sqrt{\frac{2\alpha}{M_c}} \sqrt{M - M_C} \tag{54}$$

giving rise to the kink in the plot. Since there is no black hole horizon for spacetimes with mass less than this critical value, there is no entropy contribution from the solid angle deficit at the origin. The only way the mass contributes to a varying action is through its impact on the cosmological horizon radius.

As with the Einstein case, the BHHM action increases with the remnant mass, indicating a larger remnant black hole slows down the transition, and including a black hole seed lowers the action, indicating a catalysis of the HM process. Figures 3 and 4 show the modified BHHM instanton actions in 5D and 6D, respectively. They are qualitatively the same as for the Einstein case [30], except for the mass gap in 5D. The 6D plot is representative of the situation for general higher dimensions. In both plots, solid blue lines indicate a transition to a given remnant mass and the cyan line to no remnant mass. The red line corresponds to the cosmologically equal area limit and the dots to tunnelling from a pure dS false vacuum.
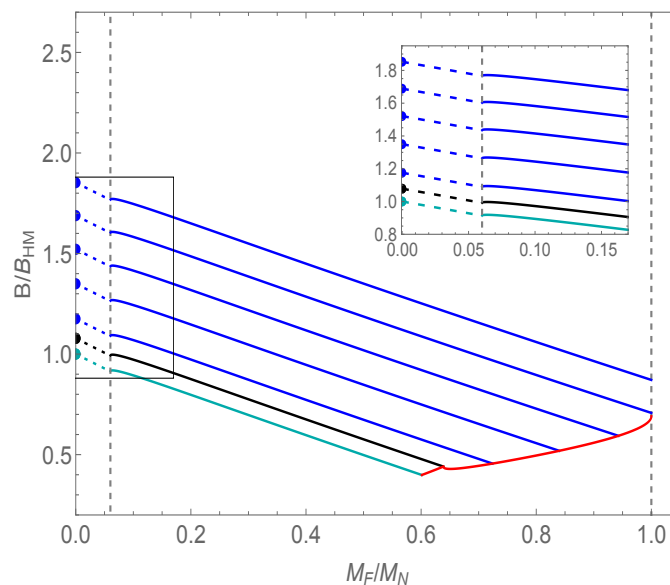

Figure 3. B/B_{HM} as a function of seed mass in 5D for parameter values $\ell_F = 5$, $\ell_T = 4.5$, and $\alpha = 0.2$, where the mass gap is $M_C \approx 0.06M_N$. The black line indicates M_C. (Figure 2 from [33]).
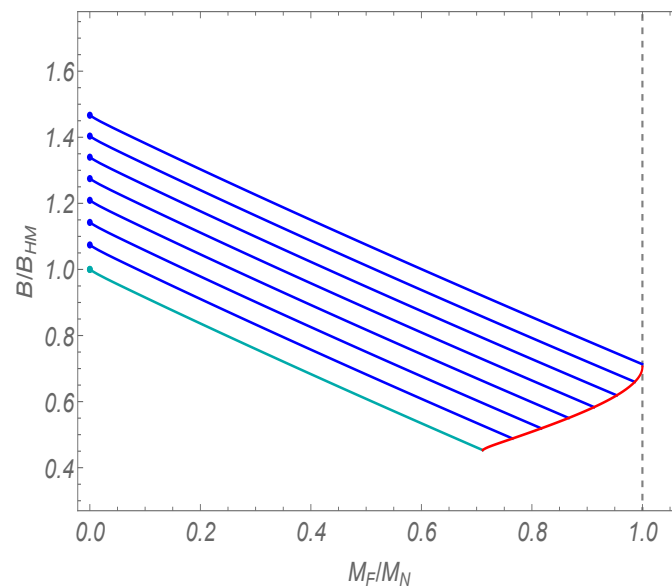
Figure 4. B/B_{HM} as a function of seed mass in 6D shown for parameter values $\ell_F = 5$, $\ell_T = 4.5$ and $\alpha = 0.2$ (Figure 3 from [33]).

The Hawking–Moss instanton is in a very different category to the first-order phase transition of bubble nucleation. The formation of bubbles, while a quantum process, is readily understandable as a phase transition through analogy with common physical processes, such as boiling water. The Hawking–Moss transition, however, is best understood with a quantum cosmology interpretation. Instantaneously, the whole universe fluctuates into what intuitively seems to be a higher energy state (though, see the discussion around the thermodynamic free energy in [30]). Therefore, there is no immediate Lorentzian continuation of the process, which is best viewed as a Boltzmann-suppressed jump. Instead, one imagines that, once the universe has taken this jump, it simply continues to roll down the far side of the potential in a classical Lorentzian evolution, akin to an inflating universe.

4. Conclusions

In this paper, we reviewed and extended work on seeded tunnelling in Einstein and EGB gravity. From the Euclidean saddle point approximation, black holes considerably enhance the probability of vacuum decay, and we showed that these results are robust to the addition of higher-order Gauss–Bonnet gravitational terms in the action, as well as extra dimensions. Interestingly, a more-generic higher-order term in the gravitational action would be problematic from this Euclidean saddle point approach. The saddle point instanton computation requires a background subtraction, i.e., an evaluation of a "background" geometry with the same asymptotics as the instanton. We rely on the uniqueness of the Schwarzschild geometry to perform this subtraction; this arises due to a Birkhoff theorem for spherically symmetric backgrounds. In the absence of such a theorem, we no longer have the uniqueness of this background [46,47]. Therefore, it might be that the simplest solution in a particular higher-order theory is not, in fact, the lowest Euclidean action solution that one should be using for background subtraction.

The study of bubble nucleation in EGB gravity was presented using the thin wall approximation, as the aim was to investigate the gravitational aspects of the problem. The equations of motion obtained by using the thin wall approximation are a good approximation when the potential barrier is sharp and transitions are rapid and complete. However, Higgs vacuum decay is, in fact, an extended thick wall region in which the Higgs deviates from its false vacuum SM value; thus, the Boltzmann suppressed static branch (where the universal result (42) applies) will be the dominant saddle point decay. Given the apparently thermal nature of this instanton, a valid concern is that, if the tunnelling is taking place in a

region around a primordial black hole, then we should be taking into account the thermal corrections to the Higgs potential.

How to precisely compute the thermal effect, however, is a difficult question, as it requires going beyond the saddle point and including not only field theory corrections, but also considering the gravitational impact. There have been several studies on this problem [48–53], exploring whether the thermal fluctuations stabilise the Higgs potential and, thus, preclude decay. Qualitative arguments might indicate that tunnelling would be suppressed or removed, but these do not consider potentially critical pre-factors and do not address the gravitational aspects of the problem in detail. Alternately, studies using a Euclidean approach or in lower dimensions leave a more-mixed picture. One problem is that the thermal corrections to the Higgs potential are only part of the question; one has to consider the cosmological setting more holistically to obtain a more-physically complete picture. In [54], the decay was studied allowing for an interstellar medium, which will be impacted by the radiation from an evaporating black hole. A hot spot forms, surrounding the primordial black hole, and provides a constant (on the evaporation/tunnelling timescale) temperature higher than the universe, but lower than the Hawking temperature of the black hole. This gives rise to thermal corrections, which tend to suppress decay while the conical deficits enhance the decay rate. The realistic environment, as well as the gravitational impacts from black holes suggest that the suppression from thermal corrections is not complete.

Moving to the higher dimensions and higher curvature gravity considered here, interestingly, the GB term lowers the temperature of a black hole of a given mass relative to its Einstein value. This would further mitigate any thermal corrections to the Higgs potential, hence lessening the relevance of such corrections. We also note that, if there are any couplings of the Higgs to the GB term (analogous to the conformal couplings such as considered in [55]), then even in 4D, the GB will now acquire some dynamical input into the different decay channels; this is an interesting and open question.

Author Contributions: Conceptualization, R.G. and S.-Q.H.; methodology, R.G. and S.-Q.H.; formal analysis, R.G. and S.-Q.H.; investigation, R.G. and S.-Q.H.; writing—original draft preparation, S.-Q.H.; writing—review and editing, R.G.; supervision, R.G.; All the authors have substantially contributed to the present work. All authors have read and agreed to the published version of the manuscript.

Data Availability Statement: Data are contained within the article.

Conflicts of Interest: The authors declare no conflicts of interest.

Abbreviations

The following abbreviations are used in this manuscript:

GR	General Relativity
GB	Gauss–Bonnet
SM	Standard Model
HM	Hawking–Moss
dS	de-Sitter
CDL	Coleman–De Luccia
BHHM	black hole Hawking–Moss

EGB   Einstein-Gauss–Bonnet
ADM   Arnowitt–Deser–Misner
SdS   Schwarzschild–de-Sitter

References

1. Clifton, T.; Ferreira, P.G.; Padilla, A.; Skordis, C. Modified Gravity and Cosmology. *Phys. Rept.* **2012**, *513*, 1–189. [CrossRef]
2. Lanczos, C. A Remarkable property of the Riemann-Christoffel tensor in four dimensions. *Ann. Math.* **1938**, *39*, 842–850. [CrossRef]
3. Zumino, B. Gravity Theories in More Than Four-Dimensions. *Phys. Rept.* **1986**, *137*, 109. [CrossRef]
4. Zwiebach, B. Curvature Squared Terms and String Theories. *Phys. Lett. B* **1985**, *156*, 315–317. [CrossRef]
5. Lovelock, D. The Einstein tensor and its generalizations. *J. Math. Phys.* **1971**, *12*, 498–501. [CrossRef]
6. Charmousis, C.; Dufaux, J.F. General Gauss–Bonnet brane cosmology. *Class. Quant. Grav.* **2002**, *19*, 4671–4682. [CrossRef]
7. Aad, G.; Abajyan, T.; Abbott, B.; Abdallah, J.; Khalek, S.A.; Abdelalim, A.A.; Aben, R.; Abi, B.; Abolins, M.; Abouzeid, O.S.; et al. Observation of a new particle in the search for the Standard Model Higgs boson with the ATLAS detector at the LHC. *Phys. Lett. B* **2012**, *716*, 1–29. [CrossRef]
8. Chatrchyan, S.; Khachatryan, V.; Sirunyan, A.M.; Tumasyan, A.; Adam, W.; Aguilo, E.; Bergauer, T.; Dragicevic, M.; Erö, J.; Fabjan, C.; et al. Observation of a New Boson at a Mass of 125 GeV with the CMS Experiment at the LHC. *Phys. Lett. B* **2012**, *716*, 30–61. [CrossRef]
9. Aad, G.; Abajyan, T.; Abbott, B.; Abdallah, J.; Khalek, S.A.; Aben, R.; Abi, B.; Abolins, M.; AbouZeid, O.S.; Abramowicz, H.; et al. Measurements of Higgs boson production and couplings in diboson final states with the ATLAS detector at the LHC. *Phys. Lett. B* **2013**, *726*, 88–119. [CrossRef]
10. Chatrchyan, S.; Khachatryan, V.; Sirunyan, A.M.; Tumasyan, A.; Adam, W.; Bergauer, T.; Dragicevic, M.; Erö, J.; Fabjan, C.; Friedl, M.; et al. Measurement of the Properties of a Higgs Boson in the Four-Lepton Final State. *Phys. Rev. D* **2014**, *89*, 092007. [CrossRef]
11. Aad, G.; Abbott, B.; Abdallah, J.; Aben, R.; Abolins, M.; AbouZeid, O.S.; Abramowicz, H.; Abreu, H.; Abreu, R.; Abulaiti, Y.; et al. Combined Measurement of the Higgs Boson Mass in pp Collisions at $\sqrt{s} = 7$ and 8 TeV with the ATLAS and CMS Experiments. *Phys. Rev. Lett.* **2015**, *114*, 191803. [CrossRef]
12. Khachatryan, V.; Sirunyan, A.M.; Tumasyan, A.; Adam, W.; Asilar, E.; Bergauer, T.; Brstetter, J.; Brondolin, E.; Dragicevic, M.; Erö, J.; et al. Measurement of the top quark mass using proton-proton data at $\sqrt{(s)} = 7$ and 8 TeV. *Phys. Rev. D* **2016**, *93*, 072004. [CrossRef]
13. Coleman, S.R. The Fate of the False Vacuum. 1. Semiclassical Theory. *Phys. Rev. D* **1977**, *15*, 2929–2936. [CrossRef]
14. Callan, C.G., Jr.; Coleman, S.R. The Fate of the False Vacuum. 2. First Quantum Corrections. *Phys. Rev. D* **1977**, *16*, 1762–1768. [CrossRef]
15. Coleman, S.R.; Luccia, F.D. Gravitational Effects on and of Vacuum Decay. *Phys. Rev. D* **1980**, *21*, 3305. [CrossRef]
16. Gibbons, G.W.; Hawking, S.W. Action Integrals and Partition Functions in Quantum Gravity. *Phys. Rev. D* **1977**, *15*, 2752–2756. [CrossRef]
17. Israel, W. Singular hypersurfaces and thin shells in general relativity. *Nuovo Cim. B* **1966**, *44*, 1–14. [CrossRef]
18. Hawking, S.W.; Moss, I.G. Supercooled Phase Transitions in the Very Early Universe. *Phys. Lett. B* **1982**, *110*, 35–38. [CrossRef]
19. Brown, A.R.; Weinberg, E.J. Thermal derivation of the Coleman-De Luccia tunneling prescription. *Phys. Rev. D* **2007**, *76*, 064003. [CrossRef]
20. Burda, P.; Gregory, R.; Moss, I. The fate of the Higgs vacuum. *J. High Energy Phys.* **2016**, *6*, 25. [CrossRef]
21. Gregory, R.; Moss, I.G.; Withers, B. Black holes as bubble nucleation sites. *J. High Energy Phys.* **2014**, *3*, 81. [CrossRef]
22. Burda, P.; Gregory, R.; Moss, I. Vacuum metastability with black holes. *J. High Energy Phys.* **2015**, *8*, 114. [CrossRef]
23. Burda, P.; Gregory, R.; Moss, I. Gravity and the stability of the Higgs vacuum. *Phys. Rev. Lett.* **2015**, *115*, 071303. [CrossRef] [PubMed]
24. Braden, J.; Johnson, M.C.; Peiris, H.V.; Pontzen, A.; Weinfurtner, S. New Semiclassical Picture of Vacuum Decay. *Phys. Rev. Lett.* **2019**, *123*, 031601. [CrossRef] [PubMed]
25. Gregory, R. Primordial Black Holes and Higgs Vacuum Decay. *Lect. Notes Phys.* **2023**, *1022*, 289–311.
26. Bowcock, P.; Charmousis, C.; Gregory, R. General brane cosmologies and their global space-time structure. *Class. Quant. Grav.* **2000**, *17*, 4745–4764. [CrossRef]
27. Gregory, R.; Padilla, A. Nested brane worlds and strong brane gravity. *Phys. Rev. D* **2002**, *65*, 084013. [CrossRef]
28. Page, D.N. Particle Emission Rates from a Black Hole: Massless Particles from an Uncharged, Nonrotating Hole. *Phys. Rev. D* **1976**, *13*, 198–206. [CrossRef]
29. Gregory, R.; Moss, I.G.; Oshita, N. Black Holes, Oscillating Instantons, and the Hawking–Moss transition. *J. High Energy Phys.* **2020**, *7*, 24. [CrossRef]
30. Gregory, R.; Moss, I.G.; Oshita, N.; Patrick, S. Hawking–Moss transition with a black hole seed. *J. High Energy Phys.* **2020**, *9*, 135. [CrossRef]
31. Cuspinera, L.; Gregory, R.; Marshall, K.; Moss, I.G. Higgs Vacuum Decay from Particle Collisions? *Phys. Rev. D* **2019**, *99*, 024046. [CrossRef]

32. Cuspinera, L.; Gregory, R.; Marshall, K.M.; Moss, I.G. Higgs Vacuum Decay in a Braneworld. *Int. J. Mod. Phys. D* **2020**, *29*, 2050005. [CrossRef]
33. Gregory, R.; Hu, S.Q. Seeded vacuum decay with Gauss–Bonnet. *J. High Energy Phys.* **2023**, *11*, 72. [CrossRef]
34. Wiltshire, D.L. Spherically Symmetric Solutions of Einstein-maxwell Theory With a Gauss–Bonnet Term. *Phys. Lett. B* **1986**, *169*, 36–40. [CrossRef]
35. Bogdanos, C. Extensions of Birkhoff's theorem in 6D Gauss–Bonnet gravity. *AIP Conf. Proc.* **2010**, *1241*, 521–527.
36. Davis, S.C. Generalized Israel junction conditions for a Gauss–Bonnet brane world. *Phys. Rev. D* **2003**, *67*, 024030. [CrossRef]
37. Wheeler, J.T. Symmetric Solutions to the Maximally Gauss–Bonnet Extended Einstein Equations. *Nucl. Phys. B* **1986**, *273*, 732–748. [CrossRef]
38. Boulware, D.G.; Deser, S. String Generated Gravity Models. *Phys. Rev. Lett.* **1985**, *55*, 2656. [CrossRef]
39. Wheeler, J.T. Symmetric Solutions to the Gauss–Bonnet Extended Einstein Equations. *Nucl. Phys. B* **1986**, *268*, 737–746. [CrossRef]
40. Myers, R.C.; Perry, M.J. Black Holes in Higher Dimensional Space-Times. *Ann. Phys.* **1986**, *172*, 304. [CrossRef]
41. Brihaye, Y.; Radu, E. Einstein-Gauss–Bonnet black holes in de-Sitter spacetime and the quasilocal formalism. *Phys. Lett. B* **2009**, *678*, 204–212. [CrossRef]
42. Clunan, T.; Ross, S.F.; Smith, D.J. On Gauss–Bonnet black hole entropy. *Class. Quant. Grav.* **2004**, *21*, 3447–3458. [CrossRef]
43. Deppe, N.; Kolly, A.; Frey, A.; Kunstatter, G. Stability of AdS in Einstein Gauss Bonnet Gravity. *Phys. Rev. Lett.* **2015**, *114*, 071102. [CrossRef]
44. Deppe, N.; Leonard, C.D.; Taves, T.; Kunstatter, G.; Mann, R.B. Critical Collapse in Einstein-Gauss–Bonnet Gravity in Five and Six Dimensions. *Phys. Rev. D* **2012**, *86*, 104011. [CrossRef]
45. Frolov, V.P. Mass-gap for black hole formation in higher derivative and ghost free gravity. *Phys. Rev. Lett.* **2015**, *115*, 051102. [CrossRef]
46. Oliva, J.; Ray, S. Birkhoff's Theorem in Higher Derivative Theories of Gravity. *Class. Quant. Grav.* **2011**, *28*, 175007. [CrossRef]
47. Kehagias, A.; Kounnas, C.; Lüst, D.; Riotto, A. Black hole solutions in R^2 gravity. *J. High Energy Phys.* **2015**, *5*, 143. [CrossRef]
48. Kohri, K.; Matsui, H. Electroweak Vacuum Collapse induced by Vacuum Fluctuations of the Higgs Field around Evaporating Black Holes. *Phys. Rev. D* **2018**, *98*, 123509. [CrossRef]
49. Hayashi, T.; Kamada, K.; Oshita, N.; Yokoyama, J. On catalyzed vacuum decay around a radiating black hole and the crisis of the electroweak vacuum. *J. High Energy Phys.* **2020**, *8*, 88. [CrossRef]
50. Shkerin, A.; Sibiryakov, S. Black hole induced false vacuum decay from first principles. *J. High Energy Phys.* **2021**, *11*, 197. [CrossRef]
51. Shkerin, A.; Sibiryakov, S. Black hole induced false vacuum decay: The role of greybody factors. *J. High Energy Phys.* **2022**, *8*, 161. [CrossRef]
52. Strumia, A. Black holes don't source fast Higgs vacuum decay. *J. High Energy Phys.* **2023**, *3*, 39. [CrossRef]
53. Briaud, V.; Shkerin, A.; Sibiryakov, S. Thermal false vacuum decay around black holes. *Phys. Rev. D* **2022**, *106*, 125001. [CrossRef]
54. Hamaide, L.; Heurtier, L.; Hu, S.Q.; Cheek, A. Primordial Black Holes Are True Vacuum Nurseries. *arXiv* **2023**, arXiv:2311.01869.
55. Rajantie, A.; Stopyra, S. Standard Model vacuum decay with gravity. *Phys. Rev. D* **2017**, *95*, 025008. [CrossRef]